CONTROL MOMENT COEFFICIENT METHODOLOGY VALIDATION FOR eVTOL SIZING

BAHRAM SOLTANMOHAMMAD[1], RUXANDRA MIHAELA BOTEZ[2]

Abstract. This paper presents a novel approach for the preliminary design of electric Vertical Takeoff and Landing (eVTOL) aircraft that utilizes the new Control Moment Coefficient (CMC) to size electric motors and to determine the rotor location and incidence angle. The CMC is determined for both thrust and arm length in eVTOL aircraft design, and is used to measure the moment produced by the rotors in the roll, pitch, and yaw axes. Analyzing its dimensionless value thus allows insights into an eVTOL aircraft's controllability. To test our methodology, two eVTOL aircraft were used in flight tests, one of which had up to 126% higher CMC values than the other. The results of the flight tests showed that a higher CMC value yielded many benefits, including an increased margin of safety between the rotors and the saturation level, reduced tracking error, and reduced control effort (or energy consumption). Furthermore, the 126% increase in the dimensionless CMC related to the pitch resulted in a 30% increase in the Pulse-Width Modulation – PWM margin of safety of the rotors at the saturated level while still maintaining a reasonable tracking error and a 97% decrease in the pitch control effort. Our research suggests that incorporating higher CMCs into the preliminary design of an eVTOL aircraft can significantly improve its safety and controllability. We hope that our findings will encourage further exploration of this promising approach in future.

Key words: eVTOL preliminary Design, Controllability, Rotor saturation, Tracking Error, Control Effort, Control Arm.

NOMENCLATURE

$Arm_{\varphi front}$ – distance (y) between front rotors and centre of gravity of aircraft;

$Arm_{\varphi back}$ – distance (y) between back rotors and centre of gravity of aircraft;

$Arm_{\theta front}$ – distance (x) between front rotors and centre of gravity of aircraft;

---

[1] PhD, Researcher, Parvaz Afraz Hava Sanat, Iran

[2] Professor, École de technologies supérieure ÉTS, University of Quebec, Canada

Ro. J. Techn. Sci. − Appl. Mechanics, Vol. 68, N^os 2–3, P. 159−179, Bucharest, 2023

DOI:10.59277/RJTS-AM.2023.2-3.05

$Arm_{\theta back}$ – distance (x) between back rotors and centre of gravity of aircraft;

$Arm_{\psi front}$ – distance (x) between the front rotor thrust projection on the horizontal axis and the center of gravity of the aircraft;

$Arm_{\psi back}$ – distance (x) between the back rotor thrust projection on the horizontal axis and the center of gravity of the aircraft;

b – wing span;

$\overline{C}$ – mean aerodynamic chord;

CMC – Control Moment Coefficient;

l_{CMC} – the roll moment produced by the rotors around the X axis;

$m-up_{CMC}$ – the pitch-up moment produced by the front rotors around the Y axis;

$m-down_{CMC}$ – the pitch-down moment produced by the back rotors around the Y axis;

n_{CMC} – the yaw moment produced by the rotors around the Z axis;

T – rotor thrust

T_{LF} – left front rotor thrust;

T_{RF} – right front rotor thrust;

T_{LB} – left back rotor thrust;

T_{RB} – right back rotor thrust;

V_h – horizontal tail volume coefficient ;

V_v – vertical tail volume coefficient ;

W – takeoff weight.

1. INTRODUCTION

In an eVTOL aircraft, the rotor thrust plays a crucial role in its control [1]. It is important to know if the rotor thrust alone is sufficient to provide hover and transition control. Hovering is the act of maintaining a fixed altitude without any forward movement. In this state, the aircraft remains completely still, with no speed in the forward direction. The move from hovering to horizontal flight is called the transition phase. During this transition phase, the forward speed gradually increases to approximately 1.2 to 1.3 times the stall speed.

A significant challenge of eVTOL designers is the appropriate sizing of an air vehicle to properly study its controllability during both hover and transition. Rotor thrust has traditionally been used to meet the lift, hover, and control requirements. In general, the amount of thrust generated by rotors is crucial in determining the size of eVTOL aircraft. This includes considering the lift required for hovering and the controllability during hovering and transitioning.

Ugwueze et al. [2] presented a robust sizing method that efficiently estimates and compares key performance parameters during the preliminary design phase for eVTOL aircraft. They employ actuator disk theory to calculate the power required in hover. In a separate study, Basset et al. [3] proposed a methodology for sizing eVTOL aircraft that addressed the most demanding flight conditions, including thruster failure. They utilized Froude's momentum theory to determine the thrust required for hover. Their research focused on investigating the effects of one or more rotor thrust failures on the maximum thrust required for eVTOL. Donateo and Çinar [4] conducted a study on optimizing aircraft configuration and propulsion system sizing to minimize power requirements during cruise. They estimated the eVTOL power demand in all flight modes, including hover and transition. Lee, Tullu, and Hwang [5] performed an optimization of an eVTOL aircraft during the preliminary design phase using the design of experiments method. They employed the momentum theory to estimate the energy required for hovering during takeoff and landing. In another paper, An et al. [6] developed a sizing methodology for a lift- and cruise-type eVTOL Unmanned Aerial Vehicle. They utilized a regression model based on existing UAV electric propulsion system data to perform the sizing. Overall, these studies contribute to the advancement of eVTOL aircraft design by providing efficient sizing methods, addressing failure scenarios, optimizing configurations, and estimating power and energy requirements.

However, the papers to date focus on thrust only for sizing purposes, neglecting the importance of rotor control in hover and transition. In reality, the control of an eVTOL aircraft is dependent upon the moment applied by the rotors, which is determined by the thrust multiplied by the distance from the center of gravity. To address this limitation, this article introduces the Control Moment Coefficient, CMC, as a new tool that incorporates both the thrust and the distance of rotors from the center of gravity. By utilizing the CMC, designers can simultaneously consider the lift and control requirements during sizing. The comparison of flight test results from two eVTOL aircraft highlights the role of CMCs in preventing errors when determining the required thrust, rotor location, and incidence angle. CMCs provide designers with a guide for determining the required thrust and the rotors' optimal location and angle. Furthermore, the similarity between the methodology of using CMCs and the use of the Tail Volume Coefficient [7] helps to make the application of CMCs simpler for designers. Overall, incorporating CMCs in eVTOL design not only enhances accuracy, it also improves the understanding and control of these eVTOLs during hover and transition.

In particular, we examine the effect of the control arm on the moments values in the three axes of roll, pitch and yaw. In the second part of this article, we examine the flight test results of two eVTOL aircraft, which differ only by the location and angle of incidence of their rotors.

In these flight tests, we examine the impact of changes to the control arm on the rotor saturation, tracking error, and control effort during hover and transition. Our results show that with an appropriate controllability criterion, we can ensure the safety and controllability of an eVTOL aircraft.

2. CONTROLLABILITY MOMENTS COEFFICIENT OR CMC

An essential requirement for each eVTOL aircraft is the ability to control itself during hover and transition flight phases, accomplished by adjusting the rotor thrust. The control of the eVTOL in hover and transition is done using the rotors' thrust and the command applied to it.

It is important to note that the moments about the $X-$, $Y-$, and $Z-$axes are not solely determined by the rotor thrust, but rather by the rotor thrust multiplied by its distance along these 3 axes to the center of gravity. In other words, the effects of the arm length and rotor thrust on moments must be considered together.

Figure 1 illustrates that both the thrust values of the rotors and their distance to the center of gravity, or thrust arm, are crucial in determining the moment value. The moment is given by $\Sigma T \times Arm$.

The CMC coefficients include:

$$l_{CMC} = \text{Roll} - \text{MC} = \frac{\left(T_{LForRF} \times Arm_{\varphi_{front}}\right) + \left(T_{LBorRB} \times Arm_{\varphi_{back}}\right)}{W \times b}, \tag{1}$$

$$m-up_{CMC} = \text{PitchUp} - \text{CMC} = \frac{T_{front} \times Arm_{\theta_{front}}}{W \times b}, \tag{2}$$

$$m-down_{CMC} = \text{PitchDown} - \text{CMC} = \frac{T_{back} \times Arm_{\theta_{back}}}{W \times b}, \tag{3}$$

$$n_{CMC} = \text{Yaw} - \text{CMC} = \frac{(T_{LF} \times Arm_{\psi_{front}}) + (T_{RB} \times Arm_{\psi_{back}})}{W \times b}. \tag{4}$$

Equations (1) to (4) show that are composed of parameters that are crucial for the design of an eVTOL. It is essential to determine the rotor's installation location and angle of incidence with respect to the vertical axes. These coefficients are similar to the and the , and so it is crucial for designers to accurately calculate the areas of both the horizontal and vertical tails during the preliminary design phase. These two areas are respectively represented by the and ratios, which also consider the distance of the empennage from the aircraft's center of gravity [7].

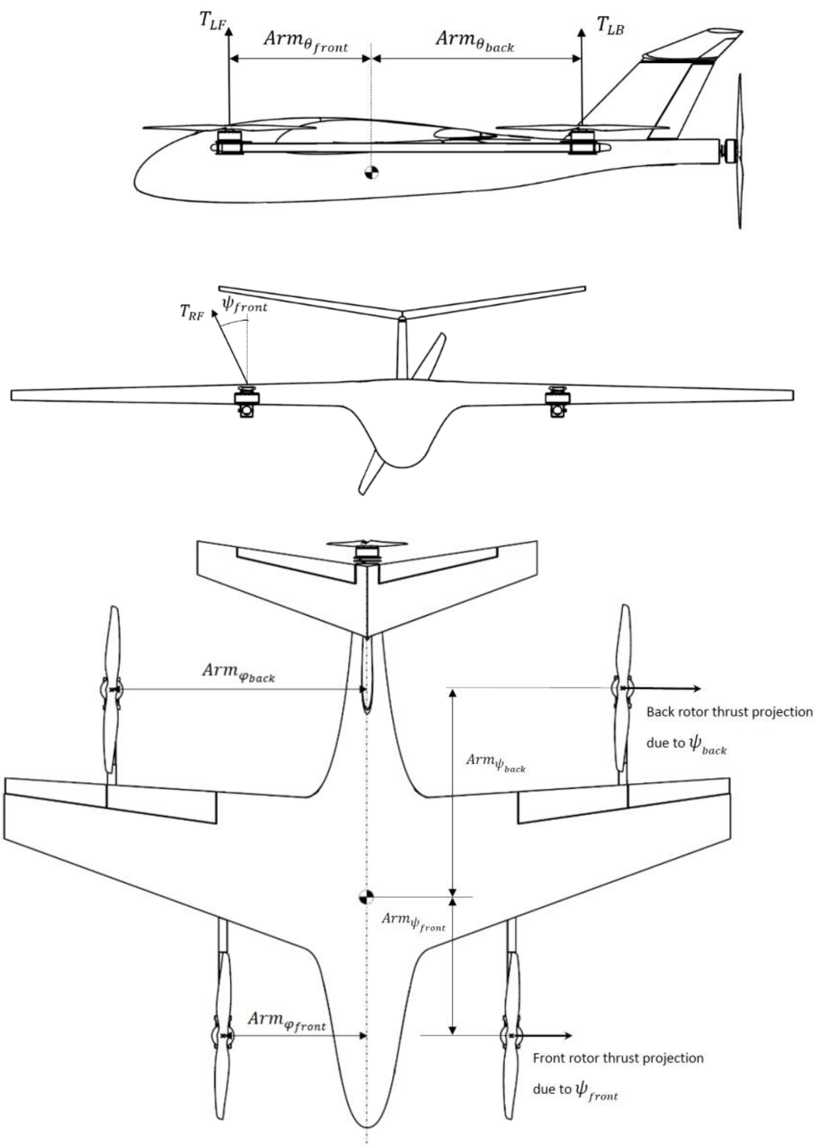

Fig. 1 – Definition of control arms on the eVTOL aircraft in 3 views (side, front and top).

eVTOL sizing can thus be designed based on the $CMCs$. Two examples illustrate this design:

1. The CMC calculation for Configuration 1, which has a trapezoidal rotor layout, Fig. 2a;

2. The CMC calculation for Configuration 2, with a rectangular rotor layout, Fig. 2b.

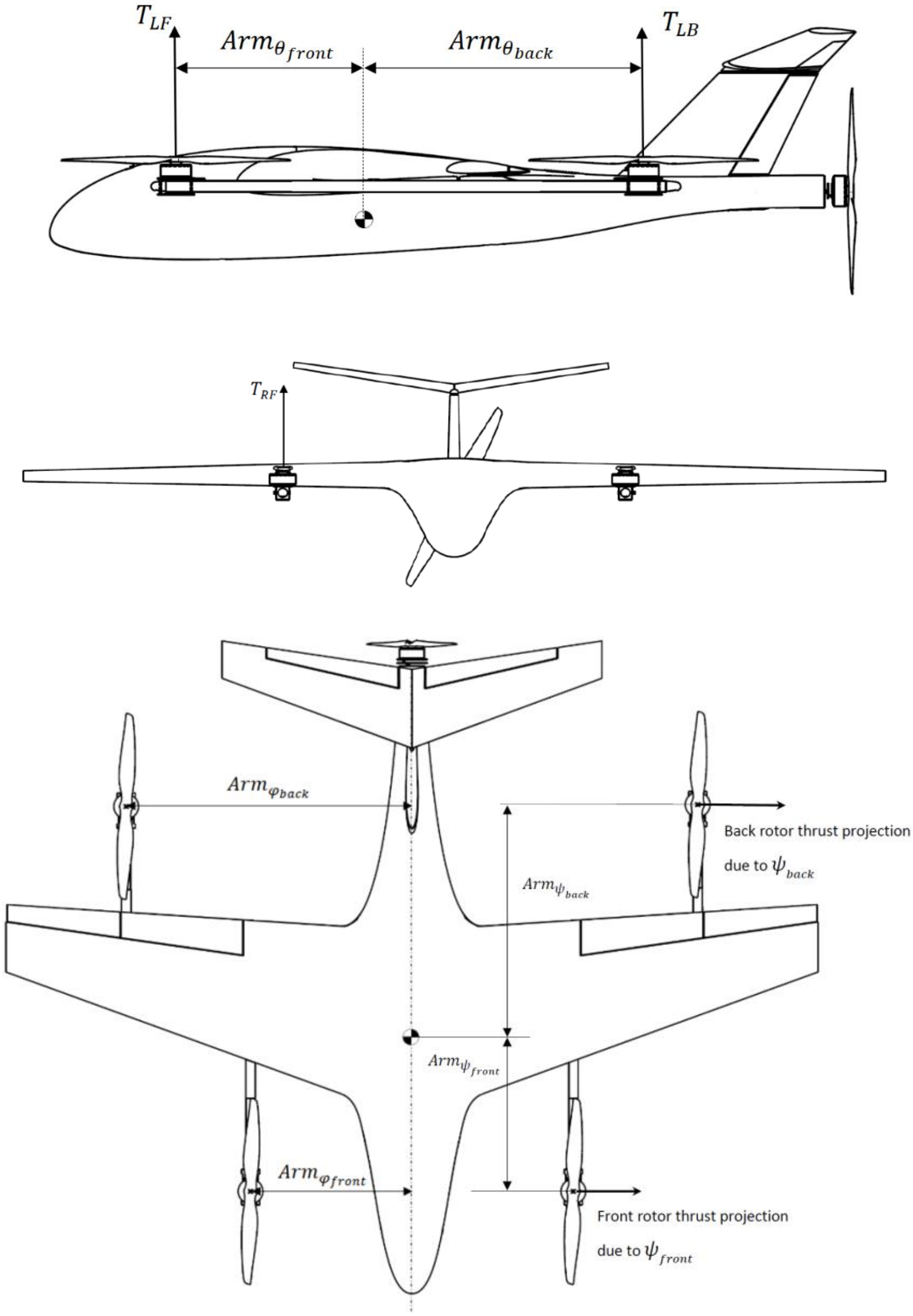

Fig. 2a – Configuration 1, three views (side, front and top).

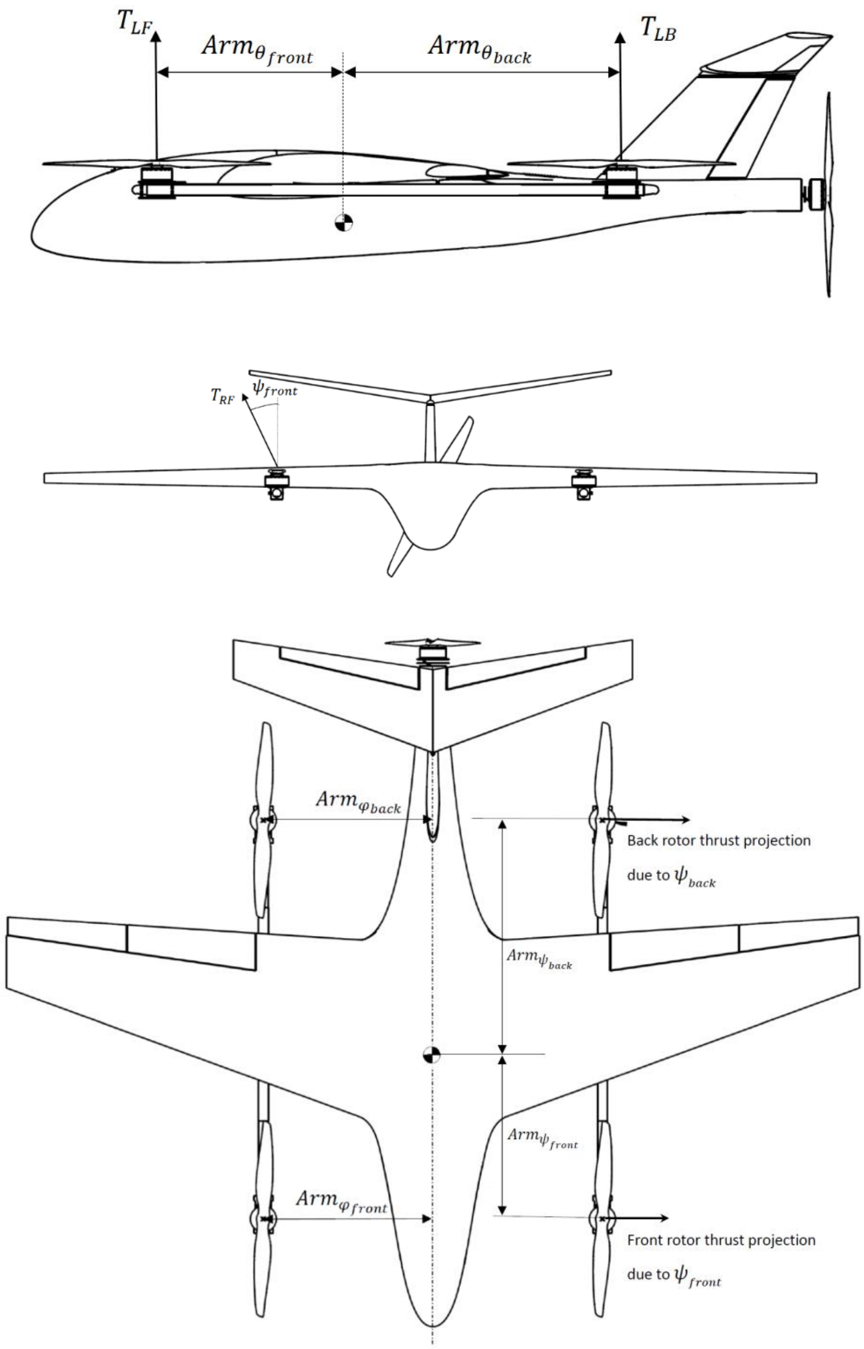

Fig. 2b – Configuration 2, three views (side, front and top).

There is a significant difference between these configurations, primarily due to their distinct layouts. Furthermore, Configuration 1 weighs 17 kilograms less than Configuration 2.

Table 1 presents the parameters and the $CMCs$ of these two configurations and highlights their differences, with the specifications for Configuration 1 in the first column, for configuration 2 in the second column, and the differences observed in Configuration 2 compared to Configuration 1 in the third column.

According to Table 1, the coefficients l_{CMC}, $m-up_{\text{CMC}}$, $m-down_{\text{CMC}}$, and n_{CMC} are all higher in Configuration 2 than in Configuration 1, while for T/W it is the reverse. This suggests that the aircraft's motion is expected to improve in its longitudinal and lateral-directional axes. However, during the transition of eVTOL aircraft, the issue of pitch-up and its control is a critical concern which needs particular attention [8, 9]. This is why $m-down_{\text{CMC}}$ coefficient has increased more than the other coefficients. As a result, the aircraft's behavior in pitch-up control is expected to improve significantly for Configuration 2.

Table 1

General specifications and *CMCs* for Configurations 1 and 2

	Configuration 1	**Configuration 2**	**Difference (%)**
W(kg)	403	420	4%
b(m)	8.3	8.3	0%
$\bar{C}$ (m)	1.5	1.5	0%
Thrust(kg)	528	528	0%
$Arm_{\varphi\,front}\,(m)$	0.544	1.557	186%
$Arm_{\varphi\,back}$ (m)	1.016	1.557	53%
$Arm_{\theta\,front}$ (m)	0.9014	1.842	104%
$Arm_{\theta\,back}$ (m)	0.9091	2.118	133%
$Arm_{\psi\,front}$ (m)	0	1.842	–
$Arm_{\psi\,back}$ (m)	0	2.118	–
Ratio&CMC			
T/W	1.31	1.26	-4%
l_{CMC}	0.12	0.23	92%
$m-up_{CMC}$	0.39	0.77	97%
$m-down_{CMC}$	0.39	0.88	126%
n_{CMC}	0	0.047	–

It should be noted that the n_{CMC} is only calculated based on the rotor angle of incidence. Therefore, the n_{CMC} for Configuration 1 is zero while for Configuration 2 it is 0.047. As a result, aircraft yaw motion is also expected to improve.

Using $CMCs$ instead of the rotor thrust allows for more careful consideration of eVTOL controllability during design. This approach can save time and cost at later design and development phases. Additionally, using CMC ensures that the rotors have the necessary margin with saturation, resulting in better command tracking and less control effort.

To confirm the proposed theory, the flight test results of two eVTOL aircraft are compared with the specifications shown in Table 1. Both configurations have very similar specifications, with the only notable differences being the location and incidence angle of the rotors, as well as a slight variation in weight. In Configuration 2, the rotor location and incidence angle are depicted in $CMCs$, showing an increase ranging from 92% to 126%, and Configuration 2 weighs 4% more than Configuration 1.

Next, we analyze the results of the flight tests on the two aircraft to determine if the theory is valid.

3. FLIGHT TEST ANALYSIS AND RESULTS

3. 1. THE EFFECT OF CMCs ON THE ROTOR'S SATURATION

Rotors are crucial components in eVTOL aircraft flight. However, as they become saturated, especially during hovering and transition, they can pose significant risks to the aircraft [10, 11]. Therefore, the margins of safety of rotor saturation levels are analyzed in two Configurations, 1 and 2. Flight tests of each configuration were carried out under virtually identical conditions. The aircraft were initially stabilized in hover before gradually increasing the throttle to 30%. However, during the flight test of Configuration 2, a lateral wind of 9 m/s caused the aircraft to change its heading and bank angles. The pilot acted on the autopilot system to quickly correct the problem.

It should be noted that Configuration 1 had a hover time of 98 seconds (Fig. 3a), with a transition time of 23 seconds (Fig. 4a), while Configuration 2 had a hover time of 61 seconds (Fig. 3b), and a transition time of 12 seconds (Fig. 4b).

Based on the data presented in Table 2 and in Fig. 3, it is evident that during hover, Configuration 1, despite being 4% lighter than Configuration 2 and having identical rotors, has an average Pulse-Width Modulation (PWM) approximately 8% higher than that of Configuration 2. In Configuration 1, the average PWM value is approximately 1 780, whereas in Configuration 2, the average PWM value is 1640. In addition, the highest PWM associated with Configuration 1 has a 10% safety margin with saturation, whereas Configuration 2 has a 16% safety margin with saturation. In conclusion, the data presented in Table 2 and in Fig. 3 provide valuable insights into the average and maximum PWM values of Configuration 1 and Configuration 2 during hover.

Table 2 and Fig. 4 show that Configuration 1 and Configuration 2 exhibit different PWM values during the transition phase. The average PWM value in Configuration 1 is 1 750. The PWM of the rear rotors increases after 3.5 seconds (Fig. 4a), red and green lines, resulting in a saturation limit of 1 900 on the left rear rotor.

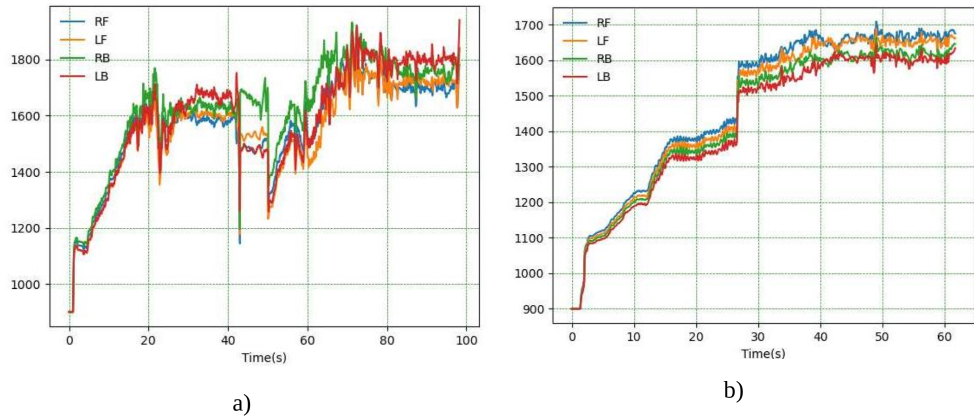

Fig. 3 – Rotors' PWM values in hover: a) Configuration 1; b) Configuration 2.

This time is indicated by a blue circle on Fig. 4a. In contrast, Configuration 2 has an average PWM value of 1650, with the highest PWM value of 1680 and a safety margin of 16%. Fig.s 3 and 4 depict the positions of the rotors, with RF representing the Right Front, LF the Left Front, RB the Right Back, and LB denoting the Left Back.

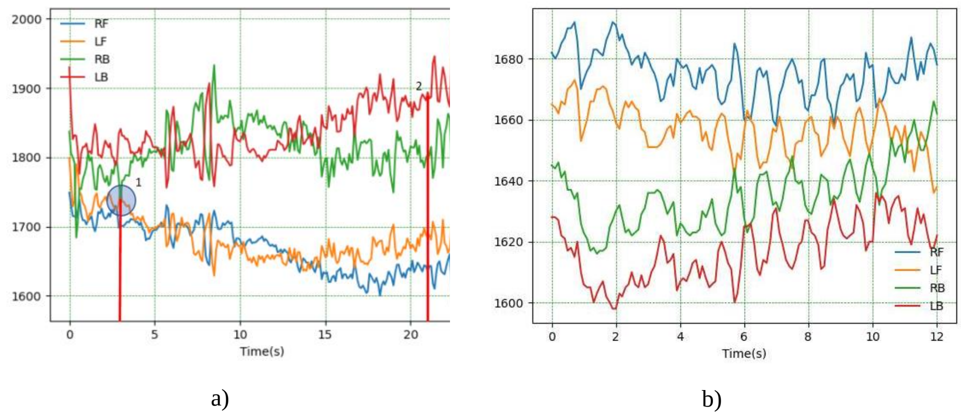

Fig. 4 – Rotors' PWM values in transition: a) Configuration 1; b) Configuration 2.

It is essential to prevent rotor saturation when controlling an eVTOL. By comparing the rotors' PWM values in Configuration 1 and Configuration 2, it is evident that increasing the CMCs will prevent rotor saturation, as Configuration 2 has a 16% safety margin. The distance from the saturation limit results in lower current consumption, which reduces energy consumption and reduces the temperature of the motor-driver-battery-wiring system.

Table 2

Difference in the PWM values of rotors in the hover and transition phases

	Hover		
	Average PWM	Max. PWM	Saturation Margin
Configuration-1	1780	1800	10%
Configuration-2	1640	1680	16%
	Transition		
	Average PWM	Max. PWM	Saturation Margin
Configuration-1	1750	2000	0%
Configuration-2	1650	1680	16%

We will delve deeper into the subject to further investigate the impact of changes in the CMCs of eVTOL aircraft.

3. 2. THE EFFECT OF CMCs ON THE DYNAMIC BEHAVIOR OF eVTOL AIRCRAFT

This section analyzes two airplanes' dynamics during flight tests. We compare their dynamics using two metrics:

Tracking Error. This metric involves designing the control input u so that the controlled output $y(t)$ tracks a given reference signal $r(t)$ despite system uncertainties. The Tracking Error [12–14] measures how well the aircraft follows the reference signal.

$$e_y(t) = y(t) - r(t). \quad (5)$$

Control Effort. The concept of Control Effort has been defined in [15,16] as an essential component of the power of a control signal. This definition can also be understood in terms of control signal energy. The control effort cost function J can be expressed as follows:

$$J = \int_{t_0}^{t_f} |u(t)| dt, \quad (6)$$

t_0 is start time, t_f – end time, and $u(t)$ – control signal.

3. 2. 1. Hover phase

Figure 5 illustrates that the bank angle ϕ is tracked with a lower error in Configuration 2 than in Configuration 1. This finding is significant, as it suggests that Configuration 2 is likely more effective at accurately tracking the bank angle ϕ.

Both Configurations successfully track the pitch angle command. However, Configuration 2 shows an enhanced tracking performance with its smaller error at the end of the hover phase, as illustrated in Fig. 6b.

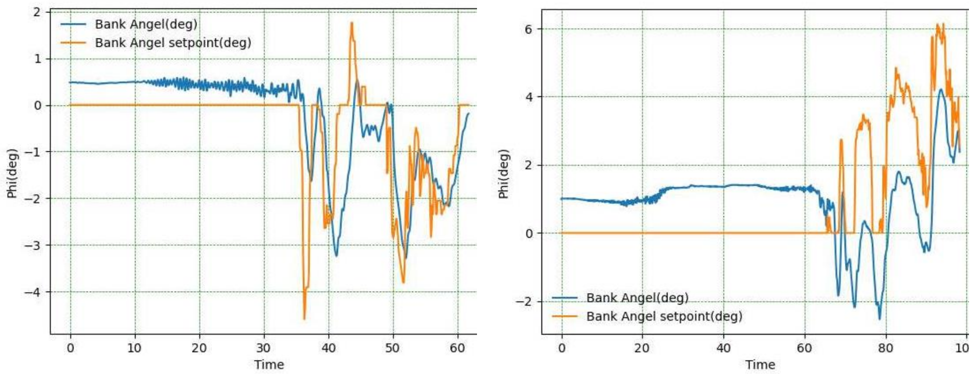

a) b)

Fig. 5 – Bank angle ϕ and its setpoint in the hover phase: a) Configuration 1; b) Configuration 2.

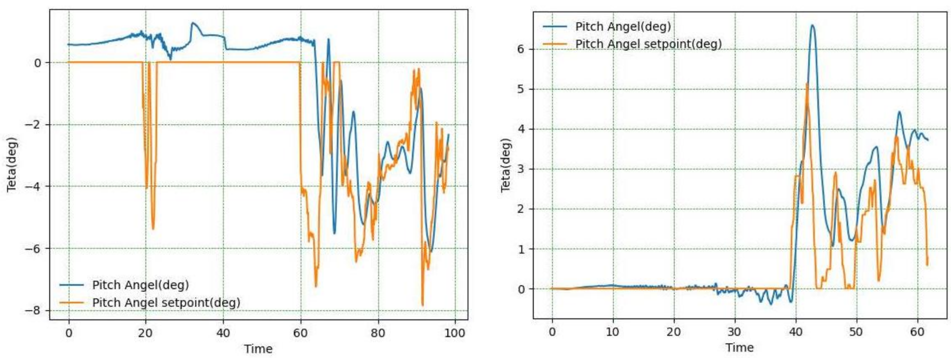

a) b)

Fig. 6 – Pitch angle θ and its setpoint in the hover phase: a) Configuration 1; b) Configuration 2.

Configuration 1 tracks the yaw command ψ but with a noticeable difference (Fig. 7a). On the other hand, Configuration 2 has 25% tracking error (Fig. 7b). Upon further analysis, it was discovered that a lateral wind at approximately 9 m/s was the underlying cause of this tracking error.

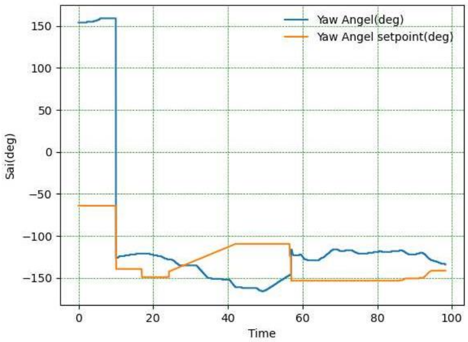

a)

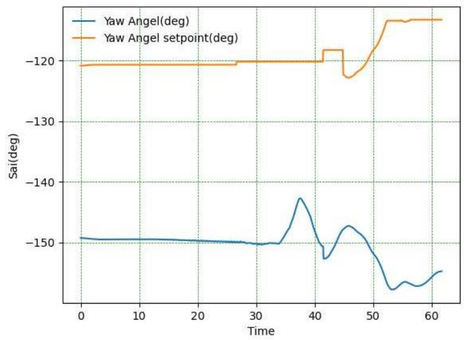

b)

Fig. 7 – Yaw angle ψ and its setpoint in the hover phase: a) Configuration 1; b) Configuration 2.

Both configurations allow control of the roll rate, with Configuration 2 requiring less control effort than Configuration 1. Specifically, the control effort in Configuration 2 is typically around 35% less than that required in Configuration-1, as shown in Table 3 and in Fig. 8a and b.

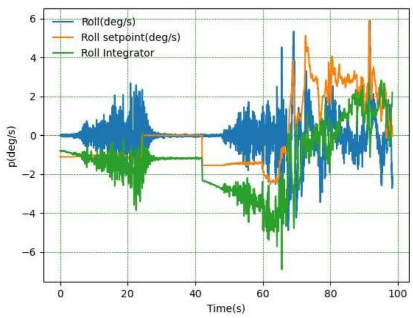

a)

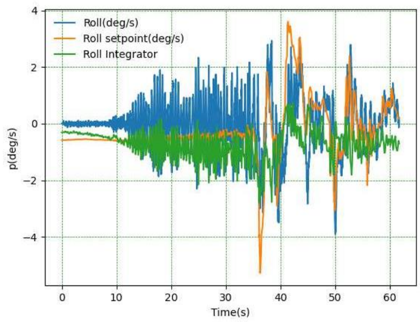

b)

Fig. 8 – Roll moment with its setpoint and its controller in the hover phase:
a) Configuration 1; b) Configuration 2.

Both configurations involve controlling the pitch rate, but in Configuration 2, control is achieved with only 34% of the control effort required in Configuration 1 (as shown in Table 3 and in Fig. 9a and b).

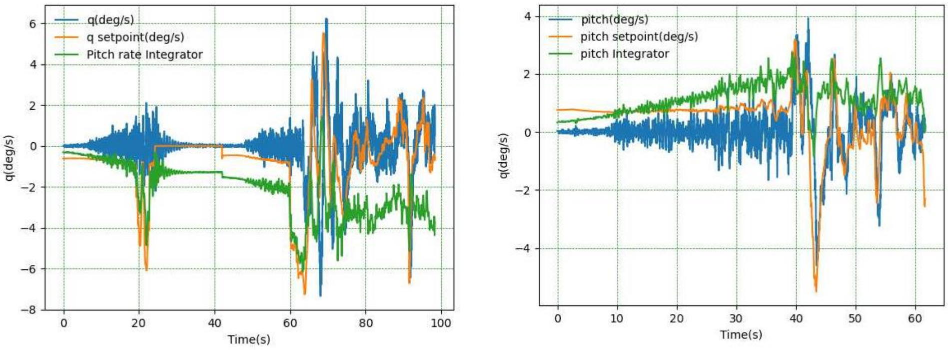

a) b)

Fig. 9 – The pitch rate *q* with its setpoint and controller in the hover phase:
a) Configuration 1; b) Configuration 2.

It is important to note that the pitch rate q is a critical parameter in this context, and accurate control is necessary to obtain optimal performance. Configuration 2's reduced control effort is a significant advantage, allowing for more efficient and cost-effective aircraft operation. This finding highlights the importance of carefully considering different configurations and their respective control requirements to achieve the most effective results.

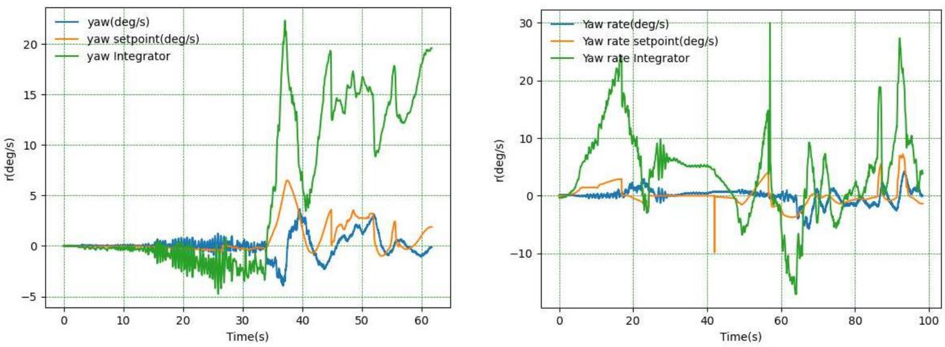

a) b)

Fig. 10 – The yaw rate with its setpoint and controller in hover:
a) Configuration 1; b) Configuration 2.

Both configurations control the yaw rate, but Configuration 2 requires a control effort of 82% compared to that of Configuration 1, as shown in Table 3 and Fig. 10a and b. Comparing the tracking errors and the control efforts reveals that increased CMCs result in the aircraft being controlled with less effort during hover, which means less energy consumption for Configuration 2, and therefore Configuration 2 better than Configuration 1.

Table 3

Control Effort in Hover

		Control Effort	Configuration 2/Configuration1
P	Configuration-1	123.06	35%
	Configuration-2	43.68	
q	Configuration-1	204.80	34%
	Configuration-2	69.33	
r	Configuration-1	403.43	82%
	Configuration-2	330.21	

3. 2. 2. Transition phase

In Configuration 1, the bank angle ϕ tracking error gradually increases after the 13th second (Fig. 11a). However, in Configuration 2, the tracking is executed with the lowest error until the end of the transition, as shown in Fig. 11b. Again, Configuration 2 demonstrates higher tracking performance than Configuration 1.

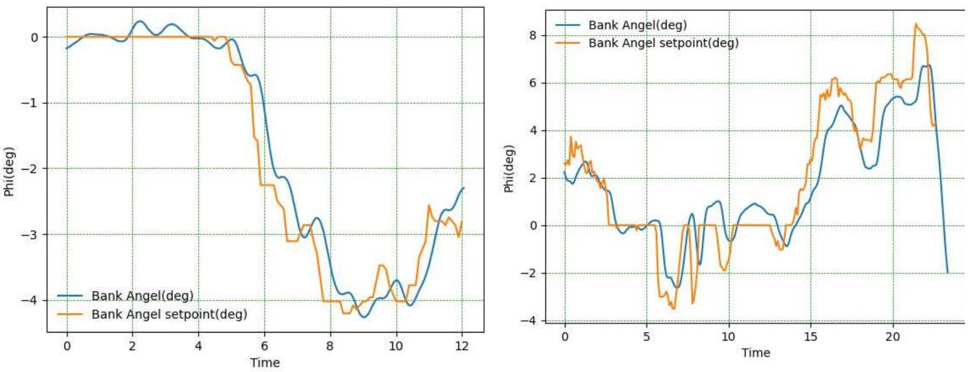

a) b)

Fig. 11 – Bank angle ϕ (deg) and its setpoint in the transition phase:
a) Configuration 1; b) Configuration 2.

As seen on Fig. 12a, in Configuration 1, the pitch angle increases significantly at 3.5 seconds (1) and then diverges at the end of the transition phase at approximate 22 seconds (2). On the other hand, in Configuration 2, the pitch angle θ drops dramatically during the first two seconds, and then reaches nearly 2 deg at the end of the transition, as shown in Fig. 12b.

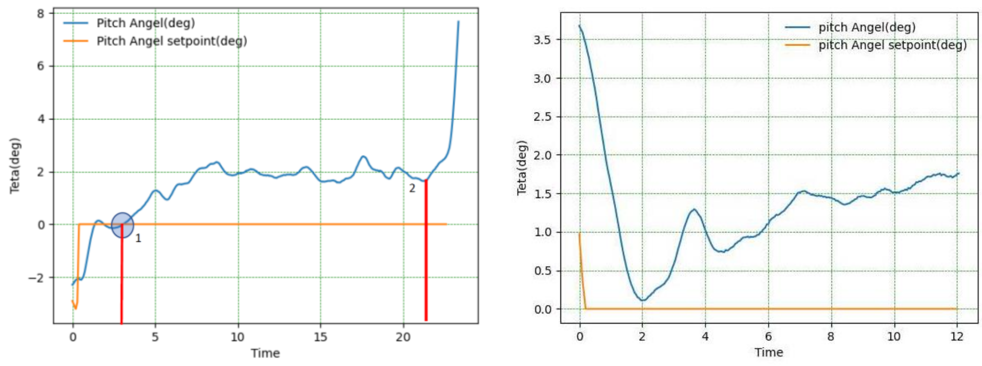

a) b)

Fig. 12 – Pitch angle (deg) and its setpoint in the transition phase:
a) Configuration 1; b) Configuration 2.

The yaw angle ψ tracking error for Configuration 1 is approximately 35 deg, as shown in Fig. 13a, while Configuration 2 exhibits a tracking error of around 40 deg (Fig. 13b). It is worth noting that the tracking error in Configuration 2 may be due to a 9m/s side wind, as illustrated in Fig. 13.

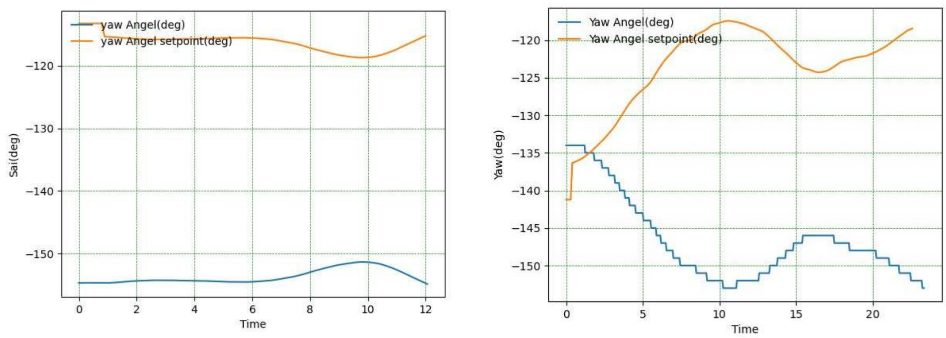

a) b)

Fig. 13 – Yaw angle ψ (deg) and its setpoint in the transition phase:
a) Configuration 1; b) Configuration 2.

Both configurations entail the controller overseeing the regulation of p. However, Configuration 1 experiences a divergence at the end of the transition, as shown in Fig. 14a, while the control effort of Configuration 2 is only 4% of the control effort of Configuration 1. This performance improvement of Configuration 2 over that of Configuration 1, as shown in Table 4 and Fig. 14(a and b), is quite significant.

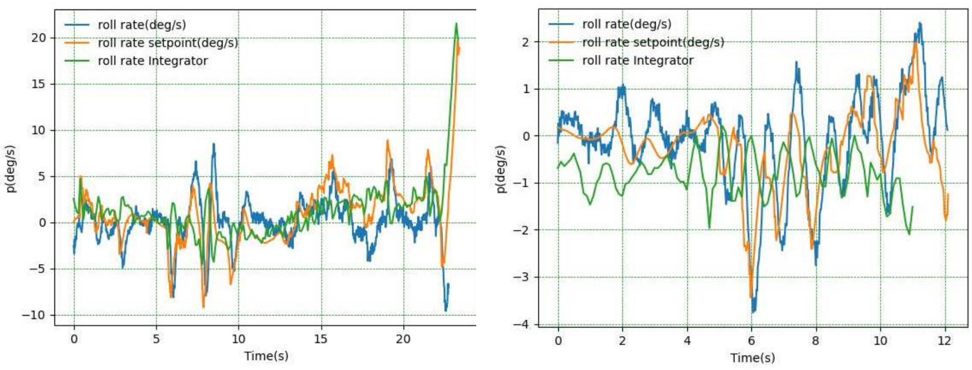

a) b)

Fig. 14 – Roll rate *p* (deg/s) with its setpoint and integrator in the transition phase:
a) Configuration 1; b) Configuration 2.

Table 4

Control Effort in the transition phase

		Control Effort	Configuration-2/Configuration-1
P	Configuration-1	209.93	4%
	Configuration-2	8.94	
q	Configuration-1	242.44	3%
	Configuration-2	7.04	
r	Configuration-1	195.84	80%
	Configuration-2	157.5	

In Configuration 1, the tracking error of the pitch rate q gradually increases after 3.5 seconds, leading to divergence at the end of the transition (Fig. 15a). However, in Configuration 2, with a relatively small control effort, the tracking error q at the end of the transition reaches a maximum of 2 deg/s, and approaches zero. This result is obtained for Configuration 2 with only a 3% control effort q compared to that of Configuration 1, as shown in Table 4 and Fig. 15(a and b). Therefore, the Configuration 2 outperforms Configuration 1 in terms of control effort and tracking error q.

In Configuration 2, the tracking error of the yaw rate r has a small increase at the end of the transition. However, the r control is executed in Configuration 2 with only 80% of the control effort compared to Configuration 1, as shown in Table 4 and Fig. 16(a and b).

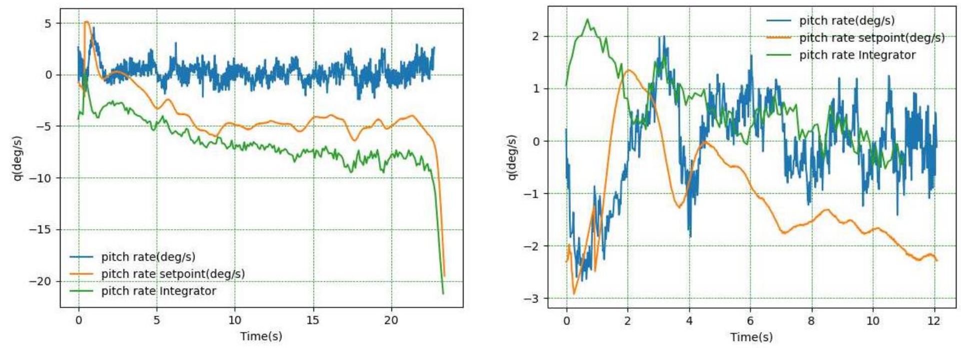

a) b)

Fig. 15 – Pitch rate *q* (deg/s) with its setpoint and integrator in the transition phase:
a) Configuration 1; b) Configuration 2.

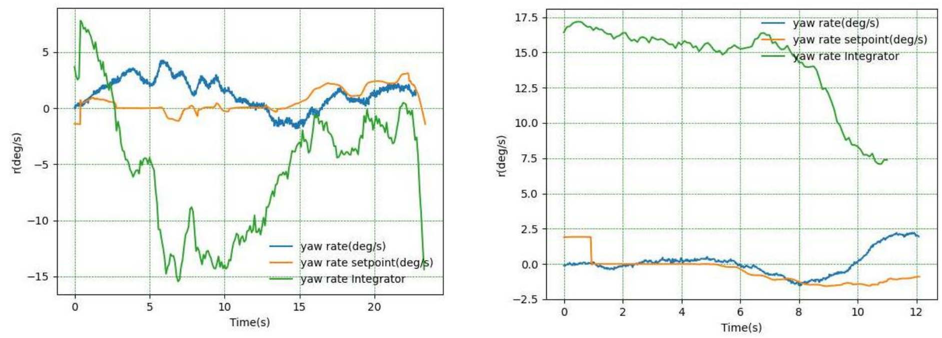

a) b)

Fig. 16 – Yaw rate *r* (deg/s) with its setpoint and integrator in the transition phase:
a) Configuration 1; b) Configuration 2.

The increase in CMC values not only prevented Configuration 2 from diverging during the transition phase, it also resulted in lower roll, pitch, and yaw control efforts than those required in Configuration 1. As a result of this improvement in control efficiency, the energy consumption was reduced. Additionally, enhancing the overall controllability of a system makes it more reliable and efficient.

4. CONCLUSION

This article proposes using CMCs in eVTOL aircraft preliminary design to size their propulsion system. These CMCs are the moment coefficients produced by rotors around their axes. These coefficients are dependent on the rotors' thrust, their distance from the eVTOL aircraft's center of gravity, and their rotors' incidence angle. The results were analyzed and it was found that increasing CMCs without changing the rotor thrust offers several benefits.

– In Configuration 2, in which $m-down_{CMC}$ was increased by 126% from this value in Configuration 1, the rotors have a reasonable safety margin from the saturation level (Table 1). The distance of 16% from the saturation level increases the safety margin in emergencies (Fig. 3 and Table 2). Moreover, the longer the distance between the rotors and the saturation level, the lower the energy consumption and thus the lower the temperature in motors, drivers, batteries, and wiring.

– Increasing the $CMCs$ hassled to lower tracking errors in hover and in the transition phase. The most significant advantage of increasing CMCs is related to the pitch angle in transition, as higher CMC values prevents pitch divergence and rotor saturation. In Configuration 1, the pitch angle θ diverges at the end of the transition, while in Configuration 2, the pitch angle reaches a maximum of 2 degrees at the end of the transition (Fig. 4).

– The increase of CMC values in Configuration 2 resulted in less control effort being required by the aircraft. The energy savings in both hover and transition are quite significant. Most of the energy savings in Configuration 2 was achieved in the pitch angle, in both hover and transition, of 66% and 97%, respectively, compared to Configuration 1. The lowest savings in control effort were noted with respect to the yaw rate in Configuration 2, Figs. 5 to 16 and Tables 3 and 4.

– Incorporating CMCs in eVTOL aircraft preliminary design can reduce or eliminate the need for design iterations due to inadequate controllability. By selecting the appropriate thrust levels, rotor locations, and incidence angles during the preliminary design, CMCs can be maintained within acceptable limits, which ensures eVTOL controllability. This approach streamlines the design process and enhances the overall efficiency of eVTOL development.

In conclusion, incorporating CMCs in eVTOL preliminary design can yield numerous advantages, including enhanced safety margins, reduced energy consumption, lower component temperatures, and decreased tracking errors, thereby helping to prevent pitch divergence and rotor saturation, as well as cost and time savings in the design process.

5. FUTURE WORK

- Determine the appropriate range for CMCs in Lift-cruise fixed-wing eVTOL aircraft:

– By conducting a statistical analysis of Lift-Cruise fixed-wing eVTOL aircraft, we can determine the suitable range for CMC values: l_{CMC}, $m-up_{CMC}$,

$m-down_{CMC}$, n_{CMC}. This information is crucial to the preliminary design of these types of eVTOLs.

To ensure optimal eVTOL performance and safety, it is essential to determine the appropriate range for $CMCs$ and their related parameters. By analyzing Lift-Cruise fixed-wing eVTOL data, we can obtain valuable insights into the ideal range of these parameters. This information can be used for the design process, resulting in more efficient and effective eVTOLs.

• Determine the Optimal range for the $CMCs$ of Tilt-Wing and Tilt-Rotor eVTOL aircraft:

The horough examination and analysis of Tilt-Wing and Tilt-Rotor eVTOL aircraft should make it possible to determine the optimal range for l_{CMC}, $m-up_{CMC}$ $m-down_{CMC}$, and n_{CMC}. These values could then be used in the preliminary design of these eVTOLs. This effort will involve a careful analysis of the data to extract all the relevant information. We expect this effort to provide valuable insights into the ideal range for eVTOL aircraft, which will certainly benefit the aviation industry.

Received on November 13, 2023

REFERENCES

1. AKASH, A., RAJ V, S., SUSHMITHA, R., PRATEEK, B., ADITYA, S., SREEHARI, V.M., *Design and Analysis of VTOL Operated Intercity Electrical Vehicle for Urban Air Mobility*, Electronics, **11**, *20*, 2022.
2. UGWUEZE, O., STATHEROS, T., HORRI, N., BROMFIELD, M.A., SIMO, J., *An Efficient and Robust Sizing Method for eVTOL Aircraft Configurations in Conceptual Design*, Aerospace, **10**, *3* ,2023.
3. BASSET, P.M., VU, B.D., BEAUMIER, P., REBOUL, G., ORTUN, B., *Models and Methods at ONERA for the Presizing of eVTOL Hybrid Aircraft Including Analysis of Failure Scenarios*, The AHS Forum May 14–17, 2018.
4. DONATEO, T., ÇINAR, H., *Conceptual Design and Sizing Optimization Based on Minimum Energy Consumption of Lift-Cruise Type eVTOL Aircraft Powered by Battery and Fuel Cell for Urban Air Mobility*, Journal of Physics: Conference Series, IOP Publishing, 2022.
5. LEE, B.S., TULLU, A., HWANG, H.Y., *Optimal Design and Design parameter Sensitivity Analyses of an eVTOL PAV in the Conceptual Design Phase*, Applied Sciences, **10**, *15*, 2020.
6. AN, J.H., KWON, D.Y., JEON, K.S., TYAN, M., LEE, J.W., *Advanced Sizing Methodology for a Multi-Mode eVTOL UAV Powered by a Hydrogen Fuel Cell and Battery*, Aerospace, **9**, *2*, 2022.
7. ROSKAM, J., *Airplane Design: Part II: Preliminary Configuration Design and Integration of the Propulsion System*, DAR Corporation, 2004.
8. SOBIESIAK, L.A., FORTIER-TOPPING, H., BEAUDETTE, D., BOLDUC-TEASDALE, F., DE LAFONTAINE, J., NAGATY, A., NEVEU, D., RANCOURT, D., *Modelling and Control of Transition Flight of an eVTOL Tandem tTlt-Wing Aircraft*, Proceedings of the 8th European Conference for Aeronautics and Aerospace Sciences, 2019.
9. MAO, S., GONG, Z., YE, Z., WANG, Z., GUO, T., ZHANG, C., *A Linear-Active-Disturbance-Rejection-Based Vertical Takeoff and Acceleration Strategy with Simplified Vehicle Operations for Electric Vertical Takeoff and Landing Vehicles*, Mathematics, **10**, *18*, 2022.

10. AKSOY, E., *Control Allocation for a Multi-Rotor e-VTOL Aircraft Using Blended-Inverse*, Master's thesis, Middle East Technical University, 2021.
11. SHI, X., *Intelligent Control for Fixed-Wing eVTOL Aircraft*, PhD Thesis, California Institute of Technology, 2021.
12. KIRK, D.E., *Optimal Control Theory: an Introduction*, Courier Corporation, 2004.
13. WANG, Y., WANG, X., SHEN, L., *Approximate Optimal Curve Path Tracking Control for Nonlinear Systems with Asymmetric Input Constraints*, Drones, **6**, *11*, 2022.
14. ALBERTOS, P., ANTONIO, S., *Multivariable Control Systems: an Engineering Approach*, Springer Science & Business Media, 2006.
15. FRANZE, G., MURACA, P., *Eigenvalue Assignment by Static Output Feedback: Minimizing of the Control Effort*, Proceedings of the 2000 American Control Conference. ACC (IEEE Cat. No. 00CH36334) IEEE, **1**, *6*, 2000.
16. REGIER, C.N., PIEPER, J.K., *Experimental Examination of Controller Performance versus Control Effort: Experimental Control of DC Motor Position*, Canadian Conference on Electrical and Computer Engineering, IEEE, 2005.